Unusual Entropy-Driven Affinity of *Chromobacterium violaceum* Lectin CV-IIL toward Fucose and Mannose[†,‡]

Martina Pokorná,[§,||] Gianluca Cioci,[||,⊥] Stephanie Perret,[⊥] Etienne Rebuffet,[⊥] Nikola Kostlánová,[§] Jan Adam,[§] Nechama Gilboa-Garber,[#] Edward P. Mitchell,[∞] Anne Imberty,*[,⊥] and Michaela Wimmerová*[,§]

National Centre for Biomolecular Research and Department of Biochemistry, Faculty of Science, Masaryk University, Kotlarska 2, 611 37 Brno, Czech Republic, Centre de Recherches sur les Macromolécules Végétales, CNRS (affiliated with Joseph Fourier), BP53, 38041 Grenoble cedex 09, France, and Bar-Ilan University, Ramat-Gan 52900, Israel, and ESRF Experiments Division, BP 220, F-38043 Grenoble Cedex, France

Received February 2, 2006; Revised Manuscript Received April 7, 2006

ABSTRACT: The purple pigmented bacterium *Chromobacterium violaceum* is a dominant component of tropical soil microbiota that can cause rare but fatal septicaemia in humans. Its sequenced genome provides insight into the abundant potential of this organism for biotechnological and pharmaceutical applications and allowed an ORF encoding a protein that is 60% identical to the fucose binding lectin (PA-IIL) from *Pseudomonas aeruginosa* and the mannose binding lectin (RS-IIL) from *Ralstonia solanacearum* to be identified. The lectin, CV-IIL, has recently been purified from *C. violaceum* [Zinger-Yosovich, K., Sudakevitz, D., Imberty, A., Garber, N. C., and Gilboa-Garber, N. (2006) *Microbiology 152*, 457−463] and has been confirmed to be a tetramer with subunit size of 11.86 kDa and a binding preference for fucose. We describe here the cloning of CV-IIL and its expression as a recombinant protein. A complete structure−function characterization has been made in an effort to analyze the specificity and affinity of CV-IIL for fucose and mannose. Crystal structures of CV-IIL complexes with monosaccharides have yielded the molecular basis of the specificity. Each monomer contains two close calcium cations that mediate the binding of the monosaccharides, which occurs in different orientations for fucose and mannose. The thermodynamics of binding has been analyzed by titration microcalorimetry, giving dissociation constants of 1.7 and 19 μM for α-methyl fucoside and α-methyl mannoside, respectively. Further analysis demonstrated a strongly favorable entropy term that is unusual in carbohydrate binding. A comparison with both PA-IIL and RS-IIL, which have binding preferences for fucose and mannose, respectively, yielded insights into the monosaccharide specificity of this important class of soluble bacterial lectins.

Chromobacterium violaceum is a free-living bacterium commonly found in the aquatic habitats of tropical and subtropical regions of the world. Its most visible characteristic, noticed at the end of 19th century, is the production of a deep violet pigment named violacein (*2*). This compound is of great interest because of its antibiotic activity against several tropical pathogens, including *Mycobacterium tuberculosis*, *Trypanosoma cruzi*, and several *Leishmania* species (*3*). Besides violacein and some related antibiotics, *C. violaceum* produces many other compounds of pharmaceutical or biotechnological interest (*4*) such as polyhydroxyalkanoate polymers that could be useful in the production of biodegradable plastics and cyanide that can be used to enhance gold recovery. The bacterium also has potential applications in bioremediation since it can degrade halogenated compounds. Due to the prospective biotechnological applications, the genome of *C. violaceum* strain ATCC 12472 was fully sequenced and annotated (*5*).

Although *C. violaceum* is considered as a saprophyte, it is also an occasional pathogen of humans and animals and may cause fatal septicaemia from skin lesions with many liver and lung abscesses. Most cases of human infection occur either early in childhood or in immunocompromised individuals (*6*). The high mortality rate of the infections, once declared, can be related to the unusual resistance of the bacteria to antibiotics (*7*).

Comparison of the *C. violaceum* ORFs to those of other free-living bacteria from soil reveals that 17.4% are most closely similar to ORFs of the bacterial phytopathogen *Ralstonia solanacearum* (*8*) and 9.61% to ORFs of *Pseudomonas aeruginosa* (*9*), which causes opportunistic infections in humans. A high percentage of ORFs (9.75%) also are quite similar to those of *Neisseria meningitidis* serogroup A (*10*), the causal agent of a serious human disease. Among the genes of *C. violaceum* that present orthologs in both of the

[†] This work was supported by the Ministry of Education (Contract MSM0021622413) and the Grant Agency of Czech Republic (Contract 204/03/H016), by CNRS, by the French Ministry of Research ACI Microbiologie program, and by Mizutani Foundation for Glycosciences.

[‡] The atomic coordinates and structure factors (entries 2BOI and 2BV4) have been deposited in the Protein Data Bank.

* To whom correspondence should be addressed. A.I.: telephone, +33-476037636; fax, +33-476547203; e-mail, imberty@cermav.cnrs.fr. M.W.: telephone, +420-549498166; fax, +420-549492690; e-mail, michaw@chemi.muni.cz.

[§] Masaryk University.

[||] These authors contributed equally to this work.

[⊥] CNRS (affiliated with Joseph Fourier).

[#] Bar-Ilan University.

[∞] ESRF Experiments Division.

10.1021/bi060214e CCC: $33.50
Published on Web 05/24/2006

R. solanacearum and *P. aeruginosa* genomes, one encodes the putative protein Q7NX84 that is similar to PA-IIL,[1] the lectin with a preference for fucose in *P. aeruginosa* (*11*), and to RS-IIL, the lectin with mannose preference in *R. solanacearum* (*12*). PA-IIL is a calcium-dependent tetrameric lectin with an unusually high affinity for fucose and fucose-containing glycoconjugates (*13*, *14*) and is involved in adhesion and biofilm formation (*15*). The putative lectin from *C. violaceum*, named CV-IIL, is 113 amino acids long (without the initiating methionine), and its sequence is 60 and 62% identical with the sequences of PA-IIL and RS-IIL, respectively (*16*).

The production and properties of native CV-IIL have recently been described (*1*). The lectin is produced as a quorum sensing-driven secondary metabolite, appearing concomitantly with violacein, and its formation is repressed in the *N*-acyl homoserine lactone-deprived CV026 mutant. CV-IIL was purified on a mannose−Sepharose column as a tetramer with a subunit size (~11.86 kDa) similar to those of PA-IIL (11.73 kDa) and RS-IIL (11.60 kDa). CV-IIL is able to agglutinate blood group O erythrocytes and has the following monosaccharide affinities that are very similar to those observed for PA-IIL: L-fucose (Fuc) > D-arabinose (Ara) > D-fructose (Fru) > D-mannose (Man) (while RS-IIL has a preference for mannose).

The high resolution X-ray crystal structure of PA-IIL has helped to clarify the atomic basis for the unusually high affinity between the lectin and the monosaccharide that appears to be related to the presence of two calcium ions in the sugar binding site (*17*, *18*). Further structural characterization of PA-IIL complexed with other monosaccharides demonstrated that D-mannose mimics L-fucose in the binding site, albeit with a different orientation of the sugar ring that presents the hydroxyl groups isosterically in the binding site (*19*). Comparison with the crystal structure of the RS-IIL−α-Me-mannoside complex demonstrated that a stretch of three amino acids in the binding site may be responsible for the preference for fucose over mannose (*20*).

In this study, CV-IIL was produced in its recombinant form in *Escherichia coli.* Specificity toward different monosaccharides was investigated by enzyme-linked lectin assay (ELLA) methods. The unusual thermodynamics of binding was investigated using isothermal titration microcalorimetry (ITC), while the molecular basis was investigated by determining two X-ray crystal structures of CV-IIL in complex with methyl α-L-fucopyranoside (Me-α-Fuc) and methyl α-D-mannopyranoside (Me-α-Man). Comparison with the thermodynamic and structural characteristics of related *P. aeruginosa* and *R. solanacearum* lectins is discussed.

EXPERIMENTAL PROCEDURES

Materials. All monosaccharides used in this study were purchased from Sigma-Aldrich (St. Louis, MO) except Me-α-Fuc which was purchased from Interchim (Montluçon, France).

[1] Abbreviations: CV-IIL, lectin II from *C. violaceum*; PA-IIL, lectin II from *P. aeruginosa*; RS-IIL, lectin II from *R. solanacearum*; Ara, D-arabinose; Fuc, L-fucose; Man, D-mannose; Me-α-Fuc, α-methyl L-fucopyranoside; Me-α-Man, α-methyl D-mannopyranoside; ELLA, enzyme-linked lectin assay; ITC, isothermal titration microcalorimetry.

Cloning and Production of Recombinant CV-IIL. The following oligonucleotides were used as primers: 5′-AGG AGT TCA TAT GGC TCA GCA AGG CG-3′ (26-mer) and 5′-GCG AAG CTT CAG CCC AGC GG-3′ (20-mer). The former was designed for the introduction of NdeI and the latter for HindIII restriction sites (underlined sequences), respectively. PCR was performed using Pfu polymerase (Promega) and genomic DNA from *C. violaceum* CCM 2076 = ATCC 7461 obtained from the Czech Collection of Microorganisms (CCM, Masaryk University) as a template. After digestion with NdeI and HindIII, the amplified fragment was introduced into the multiple cloning site of the pET-25(b+) vector (Novagen, Madison, WI), resulting in plasmid pET25cv2l.

E. coli Tuner (DE3) cells containing the pET25cv2l plasmid were cultured in 1 L of Luria broth at 37 °C. When the culture reached an optical density of 0.5−0.6 at 600 nm, isopropyl β-D-thiogalactopyranoside (IPTG) was added to a final concentration of 0.5 mM. Cells were harvested after incubation for 3 h at 30 °C, washed, and resuspended in 10 mL of buffer [20 mM Tris-HCl, 100 mM NaCl, and 100 μM $CaCl_2$ (pH 7.5)]. The cells were disrupted by sonication (Soniprep 150, Schoeller Instruments). After centrifugation at 10000*g* for 1 h, the supernatant was further purified on a D-mannose−agarose column (Sigma-Aldrich). The CV-IIL lectin was loaded onto the column in the equilibrating buffer [20 mM Tris-HCl, 100 mM NaCl, and 100 μM $CaCl_2$ (pH 7.5)] and then was eluted with the elution buffer [20 mM Tris-HCl, 100 mM NaCl, 100 μM $CaCl_2$, and 0.1 M D-mannose (pH 7.5)]. The purified protein was dialyzed against distilled water for 1 week (for the removal of D-mannose), concentrated by lyophilization, and stored at −20 °C.

Cloning and Production of Recombinant RS-IIL. The *rs2l* gene was amplified by PCR using genomic DNA from the *R. solanacearum* ATCC 11696 strain using the following primers: GAG ATT CAC TCC ATA TGG CTC AGC AAG GTG and CAA AGC TTG GGA ACC GAT CAG CCC AGC. The resulting PCR product was digested with NdeI and HindIII (underlined sequences correspond to their recognition sites), and the insert was subcloned into the *E. coli* pRSET A expression vector (Novagen) that was digested similarly. Cells harboring the pRSET*rs2l* plasmid were grown in LB broth containing 100 μg/mL ampicillin at 37 °C. Recombinant RS-IIL was further produced and purified as described above for CV-IIL.

Production of Recombinant PA-IIL. Recombinant PA-IIL was purified from *E. coli* BL21(DE3) containing the pET25pa2l plasmid as described previously (*18*).

ELLA Experiments. Enzyme-linked lectin assays (ELLAs) were performed as described previously (*14*). Briefly, 96-well microtiter plates (Nunc Maxisorb) were coated with recombinant CV-IIL (30 μg/mL) in carbonate buffer (pH 9.6). Plates were blocked with 3% BSA in PBS and incubated with L-fucose-biotinylated PAA (Lectinity Holding, Inc.) at 5 μg/mL in the presence of serial dilution of tested sugars. Streptavidin−peroxidase conjugate (Boerhinger-Mannheim, Mannheim, Germany) was then added, and the color was developed using the substrate kit for peroxidase, Sigma Fast OPD (Sigma-Aldrich). The reaction was stopped by adding 30% H_2SO_4, and the absorbance was read at 490 nm in a microtiter plate reader (Bio-Rad, model 680).

ITC Analysis. Titration calorimetry experiments were performed using a Microcal (Northampton, MA) VP-ITC microcalorimeter. All titrations were made in 0.1 M Tris-HCl buffer containing 30 μM $CaCl_2$ (pH 7.5) at 25 °C. Aliquots of 10 μL of each carbohydrate, dissolved in the same buffer, were added at 5 min intervals to the lectin solution present in the calorimeter cell. In the titrations, the protein concentration in the cell varied from 0.045 to 0.075 mM and from 0.1 to 0.25 mM for Me-α-Fuc and Me-α-Man, respectively. The sugar concentration in the 250 μL syringe was 10−20 times higher than the protein concentration used in the experiment (typically 0.4−0.7 mM for the high-affinity ligands, Me-α-Fuc and Me-α-Man for CV-IIL and RS-IIL, and 1.7−3.5 mM for the low-affinity ligand, Me-α-Man for CV-IIL). The temperature of the cell was kept at 25 ± 0.1 °C. Experiments for the evaluation of heating capacity were performed using similar conditions. Aliquots of 15 and 10 μL of 0.3 mM Me-α-Fuc were added at 5 and 8 min intervals for CV-IIL and PA-IIL, respectively, to the lectin solution present in the calorimeter cell. Data were collected at temperatures varying from 5 to 45 °C. Data from a control experiment performed via identical injections of monosaccharide into the cell containing only a buffer were subtracted prior to data analysis. Integrated heat effects were analyzed by nonlinear regression using a single-site binding model (Microcal Origin 7). Fitted data yielded the association constant (K_a) and the enthalpy of binding (ΔH). Other thermodynamic parameters, i.e., changes in free energy (ΔG) and entropy (ΔS), were calculated from the equation

$$\Delta G = \Delta H - T\Delta S = -RT \ln K_a$$

where T is the absolute temperature and $R = 8.314$ J mol^{-1} K^{-1}. At least two independent titrations were performed for each ligand that was tested. Linear regression analysis of enthalpy data versus temperature was used for calculation of the heat capacity (ΔC_p).

Crystallization. Lyophilized CV-IIL was dissolved in pure water at a concentration of 7 mg/mL in the presence of salts ($CaCl_2$ and $MgCl_2$, 2 mM) and sugars (Me-α-Fuc or Me-α-Man, 5 mM). The protein was crystallized by vapor diffusion using the hanging drop method. Initial crystallization trials were performed with the Jena Bioscience PEG8000 screen, which clearly indicated PEG 8000 in combination with inorganic salts as the starting conditions. Optimization of the initial conditions resulted in well-formed single crystals growing in 1 week from 2.5 μL of the protein sample mixed with 2.5 μL of 10% PEG 8000 and 0.1 M $(NH_4)_2SO_4$. For crystallization of the Me-α-Man complex, NaCl was used instead of $(NH_4)_2SO_4$. For data collection, the crystals were soaked in mother liquor containing 30% glycerol for as little time as possible and flash-cooled in liquid nitrogen.

Data Collection and Structure Determination. Atomic-resolution diffraction data were collected at ESRF beamline ID14-2 to 1.1 Å for the Me-α-Fuc complex and to 1.0 Å for the Me-α-Man complex. Diffraction data were processed with MOSFLM (*21*) and scaled and converted to structure factors using the CCP4 program suite (*22*). Both crystals belong to space group $P2_12_12$ with two protein molecules in the asymmetric unit. Two successive passes at low and high resolution, using one crystal, were collected and merged together. The phases for the structure were determined with ACORN (*23*), using the positions of four calcium ions in the asymmetric unit as a starting point. The positions of the calcium ions were determined by molecular replacement using MOLREP (*24*) and the PA-IIL (PDB entry 1GZT) monomer as the search model. The two chains were traced, and a first solvent model was made automatically by ARP/Warp (*25*) using the ACORN experimental phases. Refinement of the model was performed with REFMAC (*26*) combined with manual rebuilding with O (*27*). For the final stages of refinement, anisotropic *B*-factors were used for all atoms. Alternative conformations were inserted where necessary and their occupancies estimated according to the refined *B*-factors. The data collection and refinement statistics are listed in Table 1.

RESULTS

Expression and Purification of Recombinant Proteins. Using the pET25cv2l expression plasmid, CV-IIL was expressed in *E. coli* Tuner (DE3) with a typical yield of ∼30 mg of purified CV-IIL per liter of culture. The resulting protein was purified by affinity chromatography and moved as a sharp band of ∼11 kDa. Mass spectrometry analysis confirmed the molecular mass of 11.841 kDa, corresponding to the CV-IIL amino acid sequence lacking the initial methionine residue. The expression level of RS-IIL in *E. coli* was lower than those obtained with the other lectins with a typical yield of ∼10 mg of purified protein per liter of culture. However, the protein was found to be less stable than PA-IIL and CV-IIL, and only basic thermodynamics characterization could be carried out.

Monosaccharide Specificity of Recombinant CV-IIL. ELLA experiments conducted on recombinant CV-IIL confirmed that it has the same activity and the same binding preference as the wild-type protein studied by the inhibition of haemagglutination (*1*). The assays confirm that Fuc is superior to Ara, Man, or Fru for binding but that the differences are small, and therefore, all these free monosaccharides can be described as good ligands for CV-IIL (Table 2). The affinity is stronger for the methyl derivative of fucose, as commonly observed in protein−carbohydrate interactions. A comparison with the data obtained with PA-IIL indicates that both lectins bind preferentially to Fuc but that PA-IIL has a much stronger preference for monosaccharides with the L-galacto configuration (i.e., Fuc and Ara). While the affinity of PA-IIL for the latter is 200-fold higher than for the D-manno configuration (i.e., Man and Fru), the affinity of CV-IIL for them is only 6 times higher.

Crystal Structures of CV-IIL−Monosaccharide Complexes. The crystal structures of CV-IIL in complex with both Me-α-Fuc and Me-α-Man contain two monomers of 113 amino acids per asymmetric unit, together with four Ca^{2+} ions and two sugar residues. The overall topology of one monomer is that of a nine-stranded antiparallel β-sandwich consisting of two sheets, one with four strands and one with five. The dimer is made around a pseudo-2-fold axis of symmetry that brings the hydrophobic face of one β-sheet into close association with its counterpart. Dimers associate to form tetramers by a 2-fold axis of symmetry, creating ball-shaped structures (Figure 1) that are very similar to those described previously for the soluble lectins from *P. aeruginosa* (*17*) and *R. solanacearum* (*20*).

Table 1: Statistics for Data Collection and Refinement

	CV-IIL−Me-α-Fuc	CV-IIL−Me-α-Man
PDB entry	2BOI	2BV4
beamline	ID14-2	ID14-2
wavelength (Å)	0.934	0.934
resolution range (Å)	34.400−1.100 (1.129−1.100)[a]	23.200−1.000 (1.026−1.000)[a]
space group	$P2_12_12$	$P2_12_12$
a (Å)	51.09	50.68
b (Å)	89.84	89.50
c (Å)	46.48	46.48
total no. of observations	712652 (44825)[a]	802154 (23973)[a]
no. of unique reflections	87549 (6366)[a]	114226 (7874)[a]
completeness	100.0 (100.0)[a]	99.6 (94.4)[a]
R_{merge} (%)	7.4 (30.0)[a]	6.0 (44.0)[a]
$\langle I/\sigma(I)\rangle$	17.9 (5.6)[a]	17.6 (2.0)[a]
multiplicity	8.1 (7.0)[a]	7.0 (3.0)[a]
ACORN phasing statistics		
correlation coefficient	0.44 (66947)[a,b]	0.42 (88443)[a]
R-factor	0.41 (66947)[a]	0.45 (88443)[a]
refinement		
R_{cryst} (%)	10.2 (12.0)[a]	10.7 (26.0)[a]
R_{free} (%)	11.7 (13.7)[a]	12.3 (26.1)[a]
rms deviation		
bonds (Å)	0.014	0.014
angles (deg)	1.634	1.745
solvent content (%)	45	45
estimated coordinate error based on maximum likelihood (Å)	0.012	0.011
average *B*-factor for main chains/side chains/others (Å^2)	6.1/8.3/18.3	6.5/8.8/19.4
no. of Ramachandran outliers	0	0
no. of amino acids modeled with alternative conformations	20	26

[a] Values in parentheses refer to the highest-resolution shell. [b] Number of medium E reflections.

Table 2: Inhibitory Concentration of Various Carbohydrates Giving 50% Inhibition of Binding of CV-IIL or PA-IIL to L-Fucose-PAA-Biotin in a Microtiter Plate Assay[a]

	CV-IIL		PA-IIL	
monosaccharide	IC_{50} (μM)[b]	potency[c]	IC_{50} (μM)[b]	potency[c]
Me-α-Fuc	48	2.4	2.3	2.6
L-fucose	112	1	6	1
D-arabinose	197	0.55	67	0.09
Me-α-Man	600	0.18	nd[d]	nd[d]
D-mannose	700	0.16	1400	0.0043
D-fructose	860	0.13	1650	0.0036

[a] Standard deviations are smaller than 15% except for the PA-IIL−mannose experiments (23%). [b] IC_{50} values were determined from inhibition curves. Each value represents the mean of at least three independent measurements. [c] Potency is the reciprocal of the inhibiting concentration relative to fucose (taken to be 1.0). [d] Not determined.

In the complexes of CV-IIL with Me-α-Fuc and Me-α-Man, two Ca^{2+} ions and one sugar residue can be clearly observed in each binding site. All amino acids involved in calcium binding are strictly conserved among PA-IIL, RS-IIL, and CV-IIL, and the two close Ca^{2+} ions are bound in a similar manner. This binding involves the "calcium binding loop", via the side chains of Glu94, Asp98, Asp100, Asn102, and Asp103, a second loop through the side chain of Asn21, and also the acidic group of the C-terminal Gly113 of the other tightly associated monomer (Figure 1).

The electron density of each bound sugar is shown in Figure 2. In the CV-IIL−Me-α-Fuc complex, three of the hydroxyl groups, namely, O2, O3, and O4, participate directly in the coordination of the Ca^{2+} ions, with a special position for O3 that participates in the coordination sphere of both. These three hydroxyl groups also establish numerous hydrogen bonds with amino acids (Table 3 and Figure 1B). Ring oxygen O5 receives a hydrogen bond from the backbone nitrogen of Ala23. One water molecule plays a special role by bridging O1 and O2 of Me-α-Fuc with the backbone nitrogen atoms of two amino acids, namely, Thr97 and Asp98. Hydrophobic contacts are limited to the methyl group at C5 that lies in a shallow hydrophobic pocked limited by the side chains of Ala23 and Thr45.

Although the orientation of Me-α-Man in the other CV-IIL complex is completely different from that of Me-α-Fuc, a very similar network of hydrogen bonds is established (Table 3 and Figure 1C). O3 and O5 of Me-α-Man are in the same position as those of Me-α-Fuc, but O2 takes the place of O4 (and vice versa) and C5 the place of C1. As a result, O4, O3, and O2 are involved in calcium coordination and hydrogen bonds with the protein. The trapped water molecule observed in the Me-α-Fuc complex is conserved and connects the O4 atom to the backbone of Thr97 and Asp98. O1 and its methyl group are not involved in any contacts. Interestingly, the interaction of Me-α-Man with CV-IIL does not involve any detectable hydrophobic contacts, which is particularly unusual in protein−carbohydrate interactions. The hydroxymethyl group at C5 is observed in the three staggered conformations that have been demonstrated to occur in monosaccharides with the D-manno configuration either in crystal structures (*28*) or in solution (*29*). In monomer A, electron density indicates the occurrence of both *gt* (*gauche−trans* referring to O5 first and C4 second)

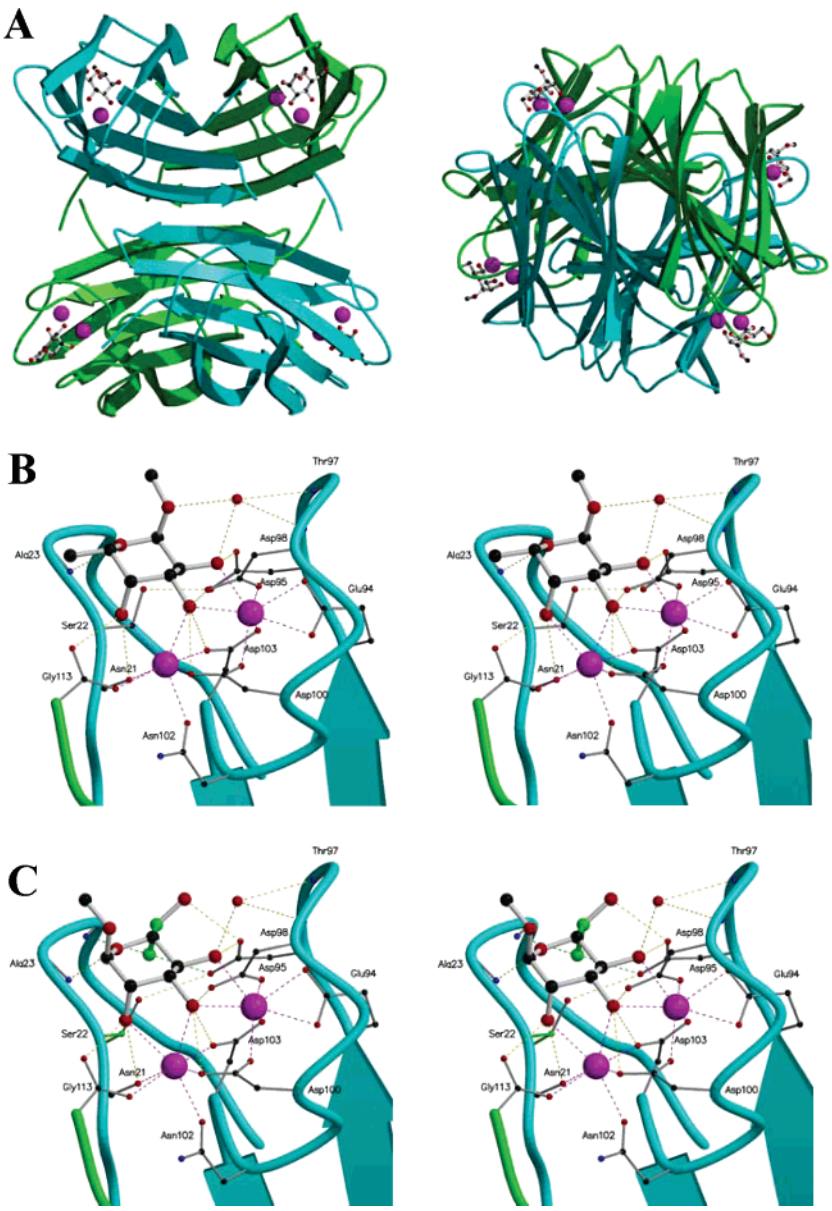

FIGURE 1: Graphical representation of CV-IIL−monosaccharide complexes. (A) Orthographic views of the tetramer of CV-IIL (ribbon) complexed with Me-α-Man (sticks) and calcium ions (CPK). (B) Stereoscopic representation of the binding site in the CV-IIL−Me-α-Fuc complex. Coordination bonds and hydrogen bonds are represented with violet and yellow dashed lines, respectively. (C) Stereo representation of the binding site in the CV-IIL−Me-α-Man complex. The alternative conformation of O6 of mannose and Ser22 are colored green. Molecular drawings were prepared with MOLSCRIPT (*39*) and RASTER-3D (*40*).

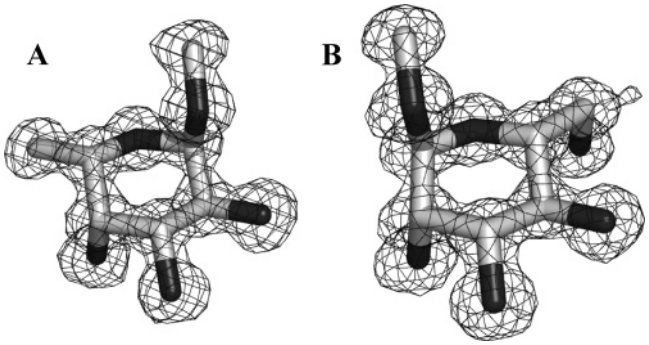

FIGURE 2: σ-weighted $2F_o - F_c$ electron density map contoured at 1σ around (A) Me-α-Fuc in the CV-IIL−Me-α-Fuc complex and (B) Me-α-Man in the CV-IIL−Me-α-Man complex.

and *gg* conformations, whereas in monomer B, the *gg* and *tg* conformations are observed. These different conformations generate different hydrogen bonding systems. While *gt* and *tg* conformations bring O6 out of the binding site, the *gg* orientation directs O6 toward the floor of the site, creating a hydrogen bond with both the backbone of Ala24 and the acidic side chain of Asp95. Interestingly, this *gg* orientation is correlated with an alternative conformation of Ser22 since it brings O6 of Me-α-Man to the position normally occupied by the hydroxyl group of this amino acid.

Thermodynamics of Binding. The result of a typical titration calorimetry measurement is shown in Figure 3. The results exhibited a monotonic decrease in the exothermic heat of the binding until saturation is achieved. The values of binding affinity K_a, binding enthalpy ΔH, and stoichiometry per monomer n have been obtained by fitting a classical equation for single-site binding (*30*). The thermodynamic parameters, free energy, and entropy of binding (ΔG and ΔS) were calculated as indicated in Experimental Procedures. The affinity constants obtained here for binding of CV-IIL

Table 3: Comparison of Contact Distances (in angstroms) in the CV-IIL Binding Site[a]

	Me-α-Fuc		Me-α-Man	
	Calcium Coordination			
Ca1	O2	2.51	O4	2.55
Ca1	O3	2.46	O3	2.49
Ca2	O3	2.48	O3	2.47
Ca2	O4	2.51	O2	2.53
	Hydrogen Bonds			
Asp95 OD1	O2	2.63	O4	2.61
Asp98 OD1	O3	2.56	O3	2.55
Asp98 OD2	O3	2.97	O3	2.99
Asp100 OD1	O3	2.92	O3	2.91
Asp100 OD2	O3	2.98	O3	2.99
Asp103 OD2	O3	3.01	O3	2.99
Asn21 O	O4	3.03	O2	3.00
Gly113* OXT[b]	O4	2.56	O2	2.58
Ala23 N	O5	3.04	O5	2.99
Ala24 N			O6-*gg*[e]	3.03
Asp95 OD2			O6-*gg*[e]	2.7
Asp95 OD1			O6-*tg*[f]	2.72
Wat_1[c]	O2	3.09	O4	2.88
Wat_1	O1	3.04		3.05
Wat_2[d]			O6A-*gt*[g]	2.87
	Hydrophobic Contacts			
Ala23 CB	$C6_{Me}$	3.85	$C1_{Me}$	3.99
Thr45 CG2	$C6_{Me}$	3.84	$C1_{Me}$	3.85

[a] Distances given are means from the distances observed in the two independent molecules in the asymmetric unit. [b] The C-terminal residue from the neighboring monomer. [c] Water bridging Thr97 NH and Asp98 NH. [d] Water bridging Asn69 ND2. [e] O6-*gg* has 30% occupancy in chain A and 70% in chain B. [f] O6-*tg* has 30% occupancy in chain B. [g] O6-*gt* has 70% occupancy in chain A.

to monosaccharides are in the micromolar range, with the highest-affinity ligand being Me-α-Fuc with a dissociation constant of 1.7×10^{-6} M (Table 4), much better than those usually observed for classical lectin−oligosaccharide interactions (*31*). The 11-fold difference between the affinity for Me-α-Fuc and that for Me-α-Man is in agreement with the relative inhibitory potencies calculated from the ELLA experiments.

PA-IIL was demonstrated before to also have high affinity for fucose (*18*) and fucose-containing oligosaccharides (*14*). When compared to PA-IIL, CV-IIL exhibits a slightly lower affinity for Me-α-Fuc, but in contrast, it is better adapted to accommodate Me-α-Man in its binding site (Table 4). The main differences between both protein−sugar interactions are shown in the thermodynamic contributions. The binding of methyl glycosides to CV-IIL is enthalpy-driven, with a ΔH of approximately −30 kJ/mol, but it also includes a strong favorable entropy contribution ($T\Delta S \sim 10$ kJ/mol) that corresponds to 34 and 41% of the free energy of binding for Me-α-Fuc and Me-α-Man, respectively. The interaction of PA-IIL with Me-α-Fuc displays different characteristics with a greater enthalpy contribution and a slightly unfavorable entropy term (*32*).

Because of the peculiar characteristics of CV-IIL−sugar interactions, further characterization of the thermodynamics was performed to determine the heat capacity change (ΔC_p) of the interaction. ITC measurements performed at temperatures varying from 5 to 45 °C demonstrated linear variations of both enthalpy and entropy contributions with temperature, but with different signs (Figure 4). The variation in enthalpy yielded a negative ΔC_p value for CV-IIL of −335 J mol^{-1} K^{-1} that is in agreement with values usually observed for

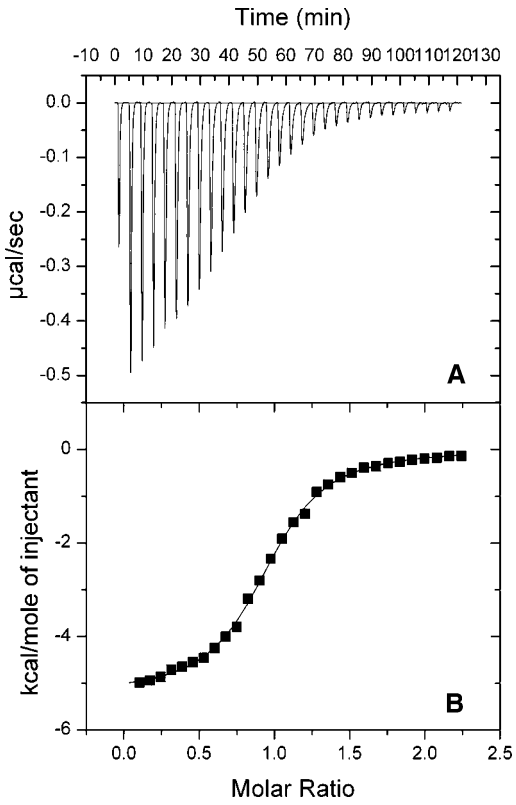

FIGURE 3: Titration microcalorimetry results for binding of Me-α-Fuc (0.4 mM) to CV-IIL (40 μM) in 0.1 M Tris buffer (pH 7.5) with 30 μM $CaCl_2$. (A) Data obtained from 30 automatic injections (10 μL) of Me-α-Fuc each into the CV-IIL-containing cell. (B) Plot of the total heat released as a function of total ligand concentration for the titration shown in panel A. The solid line represents the best least-squares fit for the obtained data.

lectin−carbohydrate interactions (*33*). The same ITC measurements performed on PA-IIL showed a similar temperature dependence in ΔH, with binding becoming more exothermic with increasing temperatures and significantly nonlinear above 30 °C. This can be explained by PA-IIL denaturation at the highest assay temperatures with the unfolding process heat adding to the binding process heat. The strong negative decline in enthalpy is compensated by higher unfavorable entropy values, resulting in almost stable free energy values. The resulting heating capacity of PA-IIL calculated from the linear part of the curve (from 5 to 25 °C) gives a value of −258 J mol^{-1} K^{-1} (Figure 4).

The relative contributions of the different thermodynamic parameters are more difficult to rationalize. The entropic term is the sum of multiple effects. A favorable entropic contribution is obtained when the increase in solvent entropy coming from water driven out of the site is correlated with a minimal loss of conformational degrees of freedom in either ligand or protein chains during binding. Chervenak and Toone (*34*) demonstrated that accurate values of ΔC_p allow determination of the different entropy contributions. Briefly, the total entropy of binding can be considered as a sum of losses in configurational and cratic (rotational and translational) entropy and changes in solvation:

$$\Delta S = \Delta S_{solv} + \Delta S_{config} + \Delta S_{rot} + \Delta S_{trans}$$

ΔS_{solv} can be expressed as follows:

Table 4: Thermodynamics of Binding of CV-IIL, PA-IIL, and RS-IIL to Me-α-Fuc and Me-α-Man As Determined by ITC at 293 K[a]

	K_A ($\times 10^4$ M^{-1})	K_D (μM)	n	$-\Delta G$ (kJ/mol)	$-\Delta H$ (kJ/mol)	$T\Delta S$ (kJ/mol)
CV-IIL						
Me-α-Fuc	59.4 ± 0.2	1.68 ± 0.01	0.95 ± 0.02	32.94 ± 0.01	21.8 ± 0.2	11.1 ± 0.1
Me-α-Man	5.4 ± 0.6	19 ± 2	0.89 ± 0.03	27.0 ± 0.3	17.8 ± 1.3	9.2 ± 1.6
PA-IIL[b]						
Me-α-Fuc	235 ± 8	0.43 ± 0.01	0.77 ± 0.03	36.4 ± 0.1	41.3 ± 1.0	−4.9 ± 1
Me-α-Man	1.42 ± 0.05	71 ± 3	0.94 ± 0.01	23.7 ± 0.1	17.8 ± 0.4	−5.9 ± 0.3
RS-IIL						
Me-α-Fuc	nd[c]					
Me-α-Man	438 ± 2	0.23 ± 0.01	0.83 ± 0.003	37.9 ± 0.1	24.9 ± 1.3	12.97 ± 0.23

[a] Standard deviations calculated from three independent measurements for both ligands. [b] Taken from ref *32*. [c] Value of $<10^4$ M^{-1}.

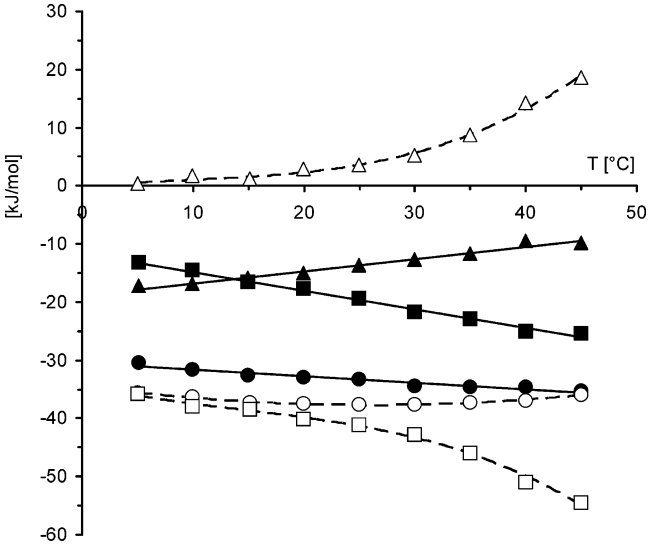

FIGURE 4: Comparison of the heat capacity plot for binding of CV-IIL (filled symbols) and PA-IIL (empty symbols) to Me-α-Fuc. The dependence of enthalpy on temperature is represented by squares together with the calculated variation of the free energy (circles) and entropy (triangles) of binding.

$$\Delta S_{solv} = \Delta S^*_{solv} + \Delta C_p \ln(T/T^*_s)$$

where T^*_s is the convergence temperature with no solvent contributions and is equal to 385.15 K. ΔS^*_{solv} covers protonation and electrostatic interactions and for lectin−sugar interactions is considered to be zero. Murphy and co-workers (*35*) proposed that the cratic contribution, for the 1:1 complex with 1M as the standard state, is equal to −33.5 J mol^{-1} K^{-1} (see refs *33* and *34* for details). On the basis of these calculations, ΔS_{solv} and, subsequently, ΔS_{config} were calculated for CV-IIL−Me-α-Fuc and PA-IIL−Me-α-Fuc interactions, respectively (Table 5). From these results, the entropy term due to the freezing of conformational freedom is significantly higher for binding of Me-α-Man to PA-IIL than to CV-IIL. This may be due to slight differences in the sequence of the protein loops involved in the binding site, causing smaller losses of mobility due to shorter or less mobile residues, and might also be correlated to the presence of one glycine residue in the carbohydrate binding loop of PA-IIL (Figure 5).

Table 5: Entropic Contribution to the Binding of Me-α-Fuc to CV-IIL and PA-IIL at 293 K

	ΔC_p (J mol^{-1} K^{-1})	ΔS (J mol^{-1} K^{-1})	ΔS_{solv} (J mol^{-1} K^{-1})	ΔS_{config} (J mol^{-1} K^{-1})
CV-IIL	−335	46.3	85.8	−6.0
PA-IIL	−258	−11.5	66.1	−44.0

DISCUSSION

Molecular Basis for Fucose versus Mannose Preference in Soluble Bacterial Lectins. The CV-IIL structure belongs to a new family of soluble bacterial lectins that also includes PA-IIL, a fucose-binding lectin (with a 200-fold lower affinity for mannose), and RS-IIL, a mannose-binding lectin (with a very low affinity for fucose). The preference of CV-IIL for fucose is only 6-fold stronger than that for mannose, and it can therefore be described as a fucose/mannose-binding lectin, i.e., with an intermediate specificity relative to those of PA-IIL and RS-IIL. Alignment of their sequences, as previously published (*16*), demonstrated that the amino acids involved in calcium binding are strictly conserved, whereas some differences are observed in the so-called "monosaccharide binding loop" in the region of amino acids 20−25 (Figure 5). The amino acids that seem to be crucial for specificity are Ser22 and Ser23 in PA-IIL, Ala22 and Ala23 in RS-IIL, and Ser22 and Ala23 in CV-IIL, which therefore appear also to be between PA-IIL and CV-IIL in terms of the degree of sequence similarity.

The resolution of the RS-IIL−mannose complex structure resulted in the conclusion that the higher affinity for mannose is due to the S22A modification since Asp95 is not involved in hydrogen bonds to Ser22 and therefore is available for bonding to O6 of mannose, yielding a higher affinity (*20*). However, the crystal structure of the CV-IIL−Me-α-Man complex presented here demonstrates that O6 of mannose is able to displace the OH group of Ser22 and to create the same hydrogen bond as in the RS-IIL−Me-α-Man complex. The two different mannose binding modes observed in the CV-IIL crystal are displayed in Figure 5. In site A, O6 is directed out of the site, because of the presence of the Ser22···Asp95 hydrogen bond, as observed in the crystal structure of the PA-IIL−mannose complex (*19*). In site B, the Ser22 hydroxyl group points in another direction and O6 can be hydrogen bound to Asp95, as observed in the crystal structure of the RS-IIL−mannose complex (*20*). Our study confirms that high affinity for mannose can be achieved only by mutation of Ser22 to an amino acid that will not make any hydrogen bonds with Asp95. This opens the route for the design of high-affinity mannose-specific lectins.

Entropy-Driven Binding of Fucosides in CV-IIL. While the binding site of CV-IIL is very similar to that of PA-IIL (Figure 5), the thermodynamics of binding is rather different. The affinity of CV-IIL for Me-α-Fuc is 6-fold lower than that of PA-IIL (Table 4), corresponding to a free energy decrease of ∼10% (−33 kJ/mol vs −36 kJ/mol). However,

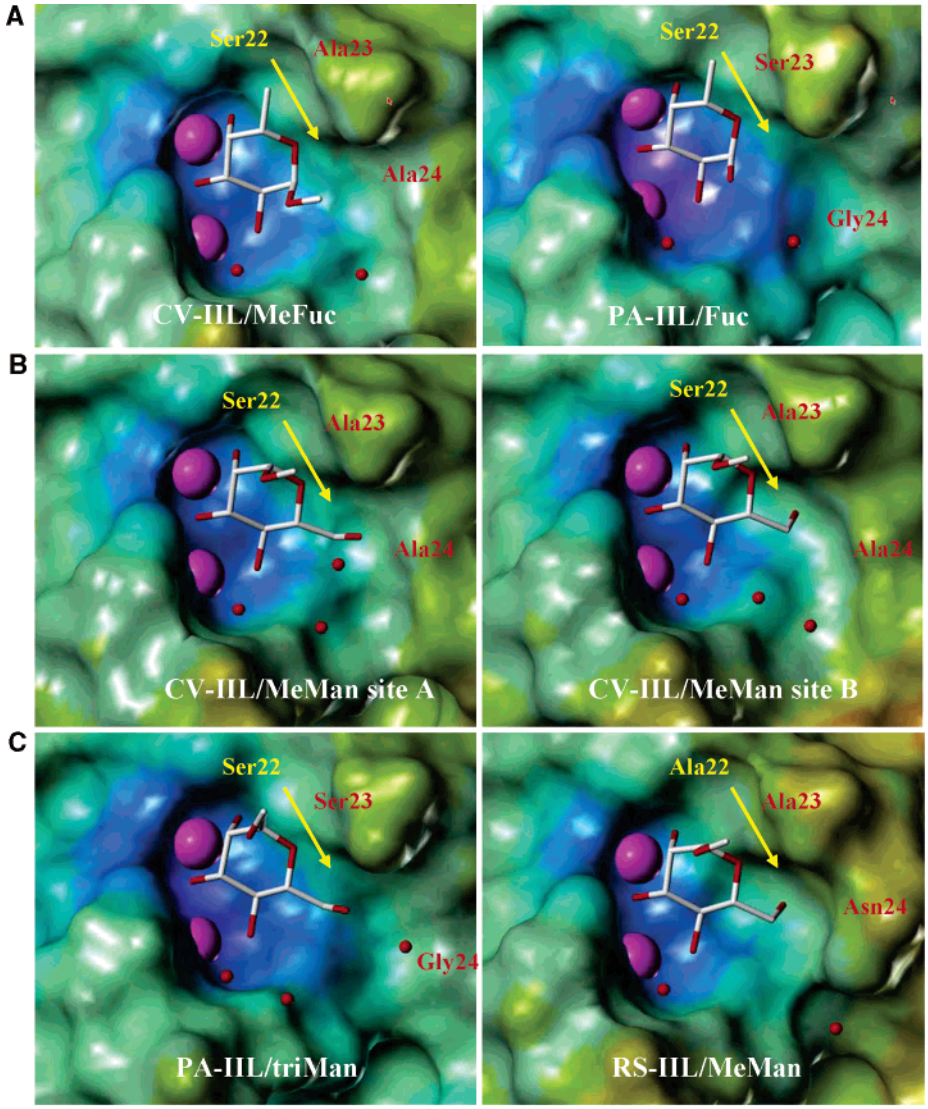

D

CV-IIL	20	VNSAATQ	25	93	SEDGTDMDYNDSI 105
PA-IIL	20	ANSSGTQ	25	94	SEDGTDNDYNDAV 106
RS-IIL	20	ANAANTQ	25	93	SEDGTDNDYNDGI 105

FIGURE 5: (A) Comparison of binding of Me-α-Fuc by CV-IIL and fucose by PA-IIL [PDB entry 1UZV (*18*)]. (B and C) Comparison of binding of Me-α-Man in the two binding sites of CV-IIL, in the binding site of PA-IIL [mannose moiety of the trimannose in PDB entry 1OVS (*19*)], and in the binding site of RS-IIL [PDB entry 1UQX (*20*)]. The accessible surfaces of the proteins have been calculated with MOLCAD (*41*) and color-coded according to the electrostatic potential from blue for negative regions to red for positive ones. (D) Comparison of sequences of the monosaccharide binding loop (residues 20−25) and the calcium binding loop (residues 93−105).

the difference is greater for the enthalpy contribution where binding of Me-α-Fuc to CV-IIL is associated with an enthalpy change of −22 kJ/mol, versus −42 kJ/mol for binding to PA-IIL. Conversely, CV-IIL has a favorable entropy contribution of approximately −11 kJ/mol at 25 °C, which corresponds to one-third of the free energy of binding. This behavior is most unusual among lectin−carbohydrate interactions that generally present a strong entropic barrier which can be attributed to either a limitation in the degrees of flexibility in the ligand (*36*) or solvent rearrangement (*37*). At present, it is difficult to correlate the thermodynamics and structural differences observed for the binding of Me-α-Fuc by CV-IIL and by PA-IIL, and further studies will be required.

Heat Capacity. The negative heat capacity observed for CV-IIL results in a less favorable enthalpy of binding at low temperatures. Nevertheless, this is offset by a positive slope for the change in the $T\Delta S$ contribution for increasing temperatures. The compensation of both enthalpy and entropy terms results in a free energy of binding that is almost independent of temperature with values varying from −31 kJ/mol at 5 °C to −36 kJ/mol at 45 °C, i.e., less than 10% variation in the scale of temperature variation that such an opportunistic organism can meet in its environment. This thermodynamic behavior could have evolved and be correlated to the high adaptability of *C. violaceum* to new environments and new hosts (*5*). PA-IIL, from *P. aeruginosa*, another highly adaptable bacterium, was also previously

demonstrated to have slightly higher agglutination activity at high temperatures (*38*). Indeed, the microcalorimetry measurement demonstrates that the PA-IIL lectin also exhibits free energy values that are almost independent of temperature, albeit with very different contributions of enthalpy and entropy.

PA-IIL, RS-IIL, and CV-IIL represent three members of a fascinating family of calcium binding lectins. As further bacterial genomes are sequenced, more instances of this family of proteins may be uncovered and lead to an improved understanding of their causative role in infection and disease.

ACKNOWLEDGMENT

The help of Laurianne Rouet is acknowledged for ELLA experiments. We thank the ESRF, Grenoble, for access to synchrotron data collection facilities.

REFERENCES

1. Zinger-Yosovich, K., Sudakevitz, D., Imberty, A., Garber, N. C., and Gilboa-Garber, N. (2006) Production and properties of the native *Chromobacterium violaceum* fucose-binding lectin (CV-IIL) compared to homologous lectins of *Pseudomonas aeruginosa* (PA-IIL) and *Ralstonia solanacearum* (RS-IIL), *Microbiology 152*, 457−463.
2. Lecoq de Boisbaudran, M. (1882) Matière colorante se formant dans la colle de farine, *C.R. Acad. Sci. 94*, 562.
3. Duran, N., and Menck, C. F. (2001) *Chromobacterium violaceum*: A review of pharmacological and industrial perspectives, *Crit. Rev. Microbiol. 27*, 201−222.
4. Stephens, C. (2004) Microbial Genomics: Tropical Treasure? *Curr. Biol. 14*, R65−R66.
5. Brazilian National Genome Project Consortium (2003) The complete genome sequence of *Chromobacterium violaceum* reveals remarkable and exploitable bacterial adaptability, *Proc. Natl. Acad. Sci. U.S.A. 100*, 11660−11665.
6. Richard, C. (1993) *Chromobacterium violaceum*, opportunist pathogenic bacteria in tropical and subtropical regions, *Bull. Soc. Pathol. Exot. Ses Fil. 86*, 169−173.
7. Fantinatti-Garboggini, F., Almeida, R., Portillo, V. A., Barbosa, T. A., Trevilato, P. B., Neto, C. E., Coelho, R. D., Silva, D. W., Bartoleti, L. A., Hanna, E. S., Brocchi, M., and Manfio, G. P. (2004) Drug resistance in *Chromobacterium violaceum*, *Genet. Mol. Res. 31*, 134−147.
8. Salanoubat, M., Genin, S., Artiguenave, F., Gouzy, J., Mangenot, S., Arlat, M., Billault, A., Brottier, P., Camus, J. C., Cattolico, L., Chandler, M., Choisne, N., Claudel-Renard, C., Cunnac, S., Demange, N., Gaspin, C., Lavie, M., Moisan, A., Robert, C., Saurin, W., Schiex, T., Siguier, P., Thebault, P., Whalen, M., Wincker, P., Levy, M., Weissenbach, J., and Boucher, C. A. (2002) Genome sequence of the plant pathogen *Ralstonia solanacearum*, *Nature 415*, 497−502.
9. Stover, C. K., Pham, X. Q., Erwin, A. L., Mizoguchi, S. D., Warrener, P., Hickey, M. J., Brinkman, F. S., Hufnagle, W. O., Kowalik, D. J., Lagrou, M., Garber, R. L., Goltry, L., Tolentino, E., Westbrock-Wadman, S., Yuan, Y., Brody, L. L., Coulter, S. N., Folger, K. R., Kas, A., Larbig, K., Lim, R., Smith, K., Spencer, D., Wong, G. K., Wu, Z., Paulsen, I. T., Reizer, J., Saier, M. H., Hancock, R. E., Lory, S., and Olson, M. V. (2000) Complete genome sequence of *Pseudomonas aeruginosa* PA01, an opportunistic pathogen, *Nature 406*, 959−964.
10. Parkhill, J., Achtman, M., James, K. D., Bentley, S. D., Churcher, C., Klee, S. R., Morelli, G., Basham, D., Brown, D., Chillingworth, T., Davies, R. M., Davis, P., Devlin, K., Feltwell, T., Hamlin, N., Holroyd, S., Jagels, K., Leather, S., Moule, S., Mungall, K., Quail, M. A., Rajandream, M. A., Rutherford, K. M., Simmonds, M., Skelton, J., Whitehead, S., Spratt, B. G., and Barrell, B. G. (2000) Complete DNA sequence of a serogroup A strain of *Neisseria meningitidis* Z2491, *Nature 404*, 502−506.
11. Gilboa-Garber, N. (1982) *Pseudomonas aeruginosa* lectins, *Methods Enzymol. 83*, 378−385.
12. Sudakevitz, D., Imberty, A., and Gilboa-Garber, N. (2002) Production, properties and specificity of a new bacterial L-fucose- and D-arabinose-binding lectin of the plant aggressive pathogen *Ralstonia solanacearum* and its comparison to related plant and microbial lectins, *J. Biochem. 132*, 353−358.
13. Imberty, A., Wimmerova, M., Mitchell, E. P., and Gilboa-Garber, N. (2004) Structures of the lectins from *Pseudomonas aeruginosa*: Insights into molecular basis for host glycan recognition, *Microb. Infect. 6*, 222−229.
14. Perret, S., Sabin, C., Dumon, C., Pokorná, M., Gautier, C., Galanina, O., Ilia, S., Bovin, N., Nicaise, M., Desmadril, M., Gilboa-Garber, N., Wimmerova, M., Mitchell, E. P., and Imberty, A. (2005) Structural basis for the interaction between human milk oligosaccharides and the bacterial lectin PA-IIL of *Pseudomonas aeruginosa*, *Biochem. J. 389*, 325−332.
15. Tielker, D., Hacker, S., Loris, R., Strathmann, M., Wingender, J., Wilhelm, S., Rosenau, F., and Jaeger, K.-E. (2005) *Pseudomonas aeruginosa* lectin LecB is located in the outer membrane and is involved in biofilm formation, *Microbiology 151*, 1313−1323.
16. Imberty, A., Mitchell, E. P., and Wimmerová, M. (2005) Structural basis for high affinity glycan recognition by bacterial and fungal lectins, *Curr. Opin. Struct. Biol. 15*, 525−534.
17. Mitchell, E., Houles, C., Sudakevitz, D., Wimmerova, M., Gautier, C., Pérez, S., Wu, A. M., Gilboa-Garber, N., and Imberty, A. (2002) Structural basis for oligosaccharide-mediated adhesion of *Pseudomonas aeruginosa* in the lungs of cystic fibrosis patients, *Nat. Struct. Biol. 9*, 918−921.
18. Mitchell, E. P., Sabin, S., Šnajdrová, L., Pokorná, M., Perret, S., Gautier, C., Hofr, C., Gilboa-Garber, N., Koca, J., Wimmerová, M., and Imberty, A. (2005) High affinity fucose binding of *Pseudomonas aeruginosa* lectin PA-IIL: 1.0 Å resolution crystal structure of the complex combined with thermodynamics and computational chemistry approaches, *Proteins: Struct., Funct., Bioinf. 58*, 735−748.
19. Loris, R., Tielker, D., Jaeger, K.-E., and Wyns, L. (2003) Structural basis of carbohydrate recognition by the lectin LecB from *Pseudomonas aeruginosa*, *J. Mol. Biol. 331*, 861−870.
20. Sudakevitz, D., Kostlanova, N., Blatman-Jan, G., Mitchell, E. P., Lerrer, B., Wimmerova, M., Katcof, F. D. J., Imberty, A., and Gilboa-Garber, N. (2004) A new *Ralstonia solanacearum* high affinity mannose-binding lectin RS-IIL structurally resembling the *Pseudomonas aeruginosa* fucose-specific lectin PA-IIL, *Mol. Microbiol. 52*, 691−700.
21. Leslie, A. G. W. (1992) Recent changes to the MOSFLM package for processing film and image plate data, *Joint CCP4 and ESF-EAMCB Newsletter on Protein Crystallography 26*.
22. Collaborative Computational Project Number 4 (1994) The CCP4 suite: Programs for protein crystallography, *Acta Crystallogr.*, 760−763.
23. Cowtan, K. D., and Zhang, K. Y. (1999) Density modification for macromolecular phase improvement, *Prog. Biophys. Mol. Biol. 72*, 245−270.
24. Vagin, A., and Teplyakov, A. (1997) MOLREP: An automated program for molecular replacement, *J. Appl. Crystallogr. 30*, 1022−1025.
25. Perrakis, A., Morris, R., and Lamzin, V. S. (1999) Automated protein model building combined with iterative structure refinement, *Nat. Struct. Biol. 6*, 458−463.
26. Murshudov, G. N., Vagin, A. A., and Dodson, E. J. (1997) Refinement of macromolecular structures by the maximum-likelihood method, *Acta Crystallogr. D53*, 240−255.
27. Jones, T. A., Zou, J. Y., Cowan, S. W., and Kjeldgaard, M. (1991) Improved methods for the building of protein models in electron density maps and the location of errors in these models, *Acta Crystallogr. A47*, 110−119.
28. Marchessault, R. H., and Pérez, S. (1979) Conformations of the hydroxymethyl group in crystalline aldohexopyranoses, *Biopolymers 18*, 2369−2374.
29. Nori, H., Nishida, Y., Ohrui, H., and Meguro, H. (1990) Conformational analysis of hydroxymethyl group of D-mannose derivatives using (6S)- and (6R)-(6-$^2H_1$)-D-mannose, *J. Carbohydr. Chem. 9*, 601−618.
30. Wiseman, T., Williston, S., Brandts, J. F., and Lin, L. N. (1989) Rapid measurement of binding constants and heats of binding using a new titration calorimeter, *Anal. Biochem. 179*, 131−137.
31. Dam, T. K., and Brewer, C. F. (2002) Thermodynamic studies of lectin-carbohydrate interactions by isothermal titration calorimetry, *Chem. Rev. 102*, 387−429.
32. Sabin, C., Mitchell, E. P., Pokorná, M., Gautier, C., Utille, J.-P., Wimmerová, M., and Imberty, A. (2006) Binding of different monosaccharides by lectin PA-IIL from *Pseudomonas aeruginosa:*

Thermodynamics data correlated with X-ray structures, *FEBS Lett. 580*, 982−987.
33. Ambrosi, M., Cameron, N. R., and Davis, B. G. (2005) Lectins: Tools for the molecular understanding of the glycocode, *Org. Biomol. Chem. 3*, 1593−1608.
34. Chervenak, M. C., and Toone, E. J. (1995) Calorimetric analysis of the binding of lectins with overlapping carbohydrate-binding ligand specificities, *Biochemistry 34*, 5685−5695.
35. Murphy, K. P., Xie, D., Thompson, K. S., Amzel, L. M., and Freire, E. (1994) Entropy in biological binding processes: Estimation of translational entropy loss, *Proteins 18*, 63−67.
36. Carver, J. P. (1993) Oligosaccharides: How flexible molecules can act as signals, *Pure Appl. Chem. 65*, 763−770.
37. Lemieux, R. U., Delbaere, L. T., Beierbeck, H., and Spohr, U. (1991) Involvement of water in host−guest interactions, *Ciba Found. Symp. 158*, 231−245.
38. Gilboa-Garber, N., and Sudakevitz, D. (1999) The hemagglutinating activities of *Pseudomonas aeruginosa* lectins PA-IL and PA-IIL exhibit opposite temperature profiles due to different receptor types, *FEMS Immunol. Med. Microbiol. 25*, 365−369.
39. Kraulis, P. (1991) Molscript: A program to produce both detailed and schematic plots of protein structures, *J. Appl. Crystallogr. 24*, 946−950.
40. Merrit, E. A., and Murphy, M. E. (1994) Raster3D version 2.0. A program for photorealistic molecular graphics, *Acta Crystallogr. D50*, 869−873.
41. Waldherr-Teschner, M., Goetze, T., Heiden, W., Knoblauch, M., Vollhardt, H., and Brickmann, J. (1992) in *Advances in Scientific Visualization* (Post, F. H., and Hin, A. J. S., Eds.) pp 58−67, Springer, Heidelberg, Germany.

BI060214E